JOTCS A
Journal of the Turkish Chemical Society
Section: A
Chemistry
TURKISH CHEMICAL SOCIETY

Photoproduction of High Molecular Weight Poly (*N*-methylpyrrole) under Green Conditions

Kerem Kaya[1]
[1] Istanbul Technical University, Chemistry Department, Istanbul, 34469, Turkey

Abstract: A novel and green photochemical polymerization method of *N*-methylpyrole is reported. Spectral and chromatographic characterizations revealed the formation of high molecular weight polymer (1436 kg/mol) having light absorption in the near-infrared region (~750 nm), high fluorescence emission in the visible region, high conductivity (0.062 S/cm) and good thermal stability. Powder X-ray diffractogram identified a totally amorphous polymer. According to cyclic voltammetry studies the polymer formed (PMPy) possess a relatively low electronic band gap (1.39 eV) which is very important for the (opto)electronic device applications of such materials.

Keywords: Conductive polymers, polypyrrole derivatives, sustainable/green chemistry, photochemical polymerization, step-growth polymerization.

Submitted: January 12, 2023. **Accepted:** April 2, 2023.

Cite this: Kaya K. Photoproduction of High Molecular Weight Poly (N-methylpyrrole) under Green Conditions. JOTCSA. 2023;10(2):443–52.

DOI: https://doi.org/10.18596/jotcsa.1232989.

***Corresponding author. E-mail:** kkaya@itu.edu.tr

1. INTRODUCTION

Following the discovery of the unprecedented conductivity of doped polyacetylene, there have been enormous studies regarding the production of the conductive polymers (CPs) for various applications (1-3). CPs can easily be structurally modified resulting in distinct physicochemical features that have found use in numerous electronic and optoelectronic devices (4-6). Especially, CPs containing heteroatoms such as polythiophene, polyaniline, polypyrrole and their derivatives have been widely used in rechargeable batteries (7), organic photovoltaics (OPVs) (8), light-emitting diodes (LEDs) (9), supercapacitators (10) and biosensors (11).

Among the heteroaromatic CPs, polypyrrole and its derivatives have attracted vast attention due to their straightforward synthesis, high conductivity and insulating properties (12, 13). Poly (*N*-methylpyrrole) (PMPy) compared to polypyrrole, has higher mechanical strength (14), better antimicrobial activity (15), higher adhesion to the metalsurfaces (16) and superior corrosion protection due to its methyl group which possesses hydrophobicity (17). Hence, PMPy and its derivatives have been recently used as anti-corrosion/anti-bacterial material (18). The dopant ions present in PMPy also play a crucial role in the hydrophobicity of the polymer (19). It is a well-known fact that anions such as hexafluorophosphate or tetrafluoroborate possess great hydrophobicity (20).

Most of the synthetic methods regarding the production of PMPy involve chemical (21, 22) and electrochemical oxidation (23-25). In chemical oxidation, excess of a hazardous transition metal salt ($FeCl_3$, $CuCl_2$, $Fe(OTs)_3$) is

usually dissolved in monomer solution of toxic organic solvents such as chloroform, dichloromethane and heated to reflux conditions for 1-2 days under inert atmosphere. Although electrochemical oxidation can be performed in short time (usually in minutes), it has several disadvantages such as the need for sophisticated electrochemical equipment, inefficiency of electrodes during polymerization and the production of very little PMPy which, most of the time, cannot be completely characterized. All these drawbacks faced in both chemical and electrochemical oxidation methods show a great barrier for the sustainable chemistry.

In the context of sustainable chemistry, light-driven chemical methods are the most favorable techniques due to the faster reaction rates, milder reaction conditions and the use of much less or no solvent (bulk photopolymerization) (26, 27). Photopolymerization reactions use only light as the input energy and don't require excess amount of toxic catalysts/solvents (28). Besides these features, photopolymerization methods possess spatiotemporal control which make them versatile for many modern applications including 3D-printing (29).

In spite of the fact that most of the photopolymerization methods concern free-radical polymerization (FRP), cationic photopolymerization reactions exhibit several advantages over their FRP counterpart including the insensitivity to air, low shrinkage and theoretical non-terminating (living) nature (30, 31). It has been previously demonstrated that cationic photopolymerization of technologically important monomers including *N*-ethylcarbazole (32, 33), thiophene (34), and thienothiophene derivatives (35) can be successfully achieved using strong photooxidants such as diphenyliodonium hexafluorophosphate (DPI).

In this work, the green photoproduction of PMPy doped with PF_6^- anions using DPI as one-component photoinitiator in ethanol solvent under near-UV irradiation and ambient conditions is reported. In contrast to insoluble polypyrrole, photoproduced PMPy showed relatively high solubility in most of the polar organic solvents (tetrahydrofuran (THF), dimethyl sulfoxide (DMSO), dimethyl formamide (DMF)). PMPy was structurally characterized using infrared (IR) and nuclear magnetic resonance (NMR) spectroscopies. According to gel-permeation chromatography (GPC), conductivity, UV-vis and fluorescence measurements, the photoproduced PMPy had high molecular weight (1436 kg/mol), high conductivity (0.062 S/cm), broad UV-vis-NIR absorption (reaching near-infrared region) and strong white light photoluminescence, respectively. Thermal stability and crystallinity of the polymer was also investigated using differential scanning calorimeter (DSC), thermogravimetric analysis (TGA) and powder X-ray diffractometry (PXRD), respectively. Cyclic voltammetry studies performed pointed out to relatively low band gap (1.39 eV) which is important for (opto)electronic utilization.

2. MATERIALS AND METHOD

2.1. Materials

N-methylpyrrole (NMPy) (Sigma-Aldrich, 99%) and diphenyliodonium hexafluorophosphate (Sigma-Aldrich, >98%) were kept in the fridge prior to use and used as received. All the other chemical reagents (solvents) including absolute ethanol (96%, Merck), methanol (Merck, 99.8%), tetrahydrofuran (Sigma-Aldrich, 99.9%), dimetylformamide (Merck, 99.8%) and dimethylsulfoxide (Merck, 99.9%) were purified according to conventional techniques prior to use.

2.2. Methods

2.2.1. Photoproduction of PMPy

PMPy was prepared by mixing 900 µL of NMPy (1 mmol) and 852 mg of DPI (2 mmol) in 2 mL of EtOH inside a test tube which was then irradiated using a photoreactor equipped with 12 lamps emitting light nominally at 355 nm (~100 mW/cm^2) for 4 h. Viscous black solution formed were then precipitated into hot n-hexane in order to remove any unreacted NMPy or DPI. After washing with ethanol, PMPy was dried under vacuum for 2 days before any characterization.

2.2.2. Gel permeation chromatography (GPC)

GPC measurements were performed on a TOSOH EcoSEC GPC system equipped with an auto-sampler system, a temperature-controlled pump, a column oven, a refractive index (RI) detector, a purge and degasser unit, and a TSKgel superhZ2000 4.6 mm ID × 15 cm × 2 cm column. Tetrahydrofuran was used as an eluent at flow rate of 1.0 mL/min at 40°C.

2.2.3. UV-vis Spectroscopy

UV-vis spectra were recorded with a Shimadzu UV-1601 double-beam spectrometer equipped with a 50 W halogen lamp and a deuterium lamp which can operate between 200 and 900 nm.

2.2.4.Fluorescence Spectroscopy
Fluorescence meausuerements were performed using Perkin-Elmer LS55 which can operate between 200 and 900 nm. with a slit width of 5 nm and 1 cm path length cuvette.

2.2.5. NMR Spectroscopy
^{1}H NMR and ^{13}C spectra were recorded in deuterated chloroform ($CDCl_3$ with tetramethylsilane as an internal standard) at 500 MHz on an Agilent VNMRS 500 spectrometer at 25° C.

2.2.6. IR Spectroscopy
Fourier-transform infrared (IR) spectra were recorded on a PerkinElmer Spectrum One spectrometer with an ATR accessory (ZnSe, PikeMiracle) and a mercury cadmium telluride (MCT) detector. A total of 32 scans were averaged.

2.2.7. Cyclic Voltammetry
The electrochemical measurements were performed by using a CH Instruments 617D potentiostat− galvanostat system. The electrochemical cell containing a Ag wire as a reference electrode (RE), a Pt wire as counter electrode (CE), and glassy carbon as a working electrode (WE) was immersed in 0.1 M tetrabutylammonium hexafluorophosphate as the supporting electrolyte under argon atmosphere.

2.2.8. Powder X-Ray Diffractography
Crystallographic identification was accomplished by X-ray diffraction (XRD) method on a benchtop Rigaku Miniflex diffractometer with a Cu-Kα radiation source operated at 30 kV and 10 mA. The acquisition angle ranged from 2° to 90°.

2.2.9. Thermal Analysis
Thermogravimetric analysis (TGA) was performed on a Perkin-Elmer Diamond TA/TGA with a heating rate of 10 K/min under constant nitrogen flow of 200 mL/min.

2.2.10. Conductivity Measurements
Conductivity measurements were performed in air at room temperature using a HP3478A digital voltmeter, with a direct 4-wire resistance capability.

3. RESULTS AND DISCUSSION

Following the photopolymerization, precipitation and drying procedures, molecular weight of obtained PMPy was investigated using GPC. The results are tabulated in Table1.

Table 1.GPC results of PMPy obtained by photopolymerization.[a]

Polymer	Conversion (%)[b]	M_n (kg/mol)[c]	$Đ^c$
PMPy	72	1436	1.37

[a]1 mmol of NMPy was mixed with 2 mmol of DPI inside a tube irradiated inside a photoreactor for 4 h. (details can be found in the materials and method section). [b]Determined gravimetrically. [c]Determined using GPC calibrated with polystyrene standards having narrow molecular weight distribution (1.05).

It is interesting to observe GPC traces (Figure 1) belonging to very high molecular weight species since similar CPs are known to have poor solubility in most of the solvents (36). This phenomenon can be attributed to the highly doped nature of PMPy resulting in increased ion-dipole interactions between dopant ions (PF_6^-) and dipole of polar organic solvents such as THF, DMSO and DMF (37). Dispersity index of 1.37 is a clear indication of the step-growth nature of the photopolymerization as similar indices were previously observed in the photoinduced step-growth polymerization of other heteroaromatics monomers (38).

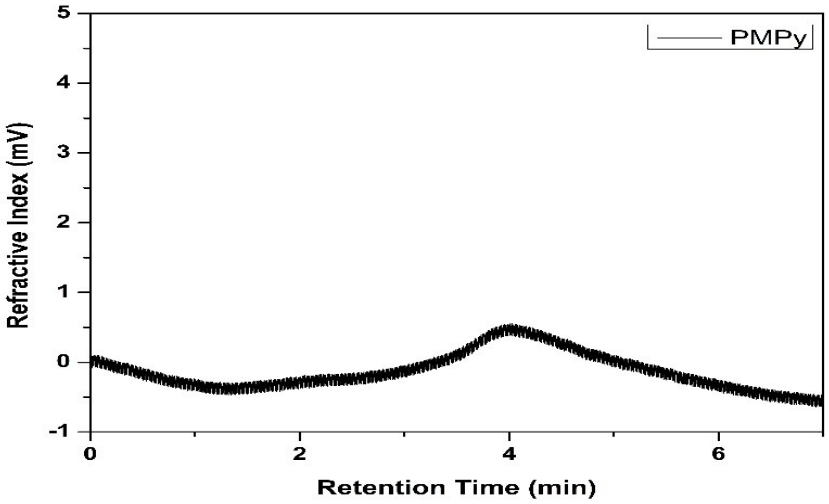

Figure 1. GPC traces of PMPy.

UV-vis absorbance spectrum of the dark colored PMPy in DMSO solvent exhibited strong bathochromic shift (~450 nm) compared to the spectrum of its monomer analogue as can be seen in Figure 2. The absorbance in the near-infrared (NIR) region confirms the presence of high molecular weight species having increased conjugation.

Figure 4a and 4b show ^{1}H and ^{13}C NMR spectra of PMPy, respectively. Clear broadening in the aliphatic region and aromatic region corresponds to *N*-methyl and pyrrole ring protons, respectively, indicating successful polymerization. In the ^{1}H NMR spectrum, the ratio of the integral areas of the aliphatic and aromatic regions are 3:6 instead for 3:2 due the low resolution caused by the insolubility of large molecular weight polymers, the end group aromatic protons of different chain length polymers and due to the presence of NMR solvent $CDCl_3$.

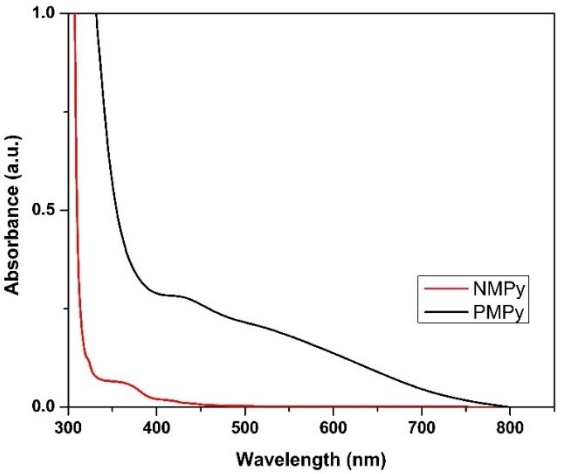

Figure 2. UV-vis spectra of (red) NMPy and black (PMPy) (solvent:DMSO).

Excitation of DMSO solution of PMPy in different wavelengths resulted in fluorescence emissons covering the whole blue-red-green zone (visible to NIR) (Figure 3). causing a strong white light luminescence, especially upon excitation at 355 nm (Figure 3 inset photo).

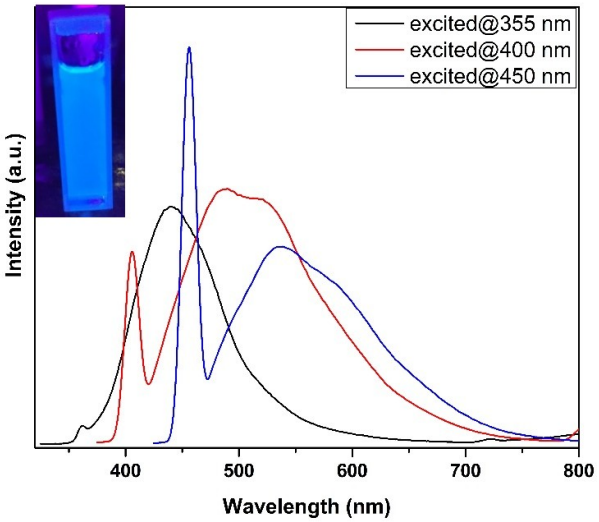

Figure 3. Fluorescence emission of PMPy excited at different wavelength (inset photo shows the white photoluminescence of PMPy excited at 355 nm) (solvent: DMSO).

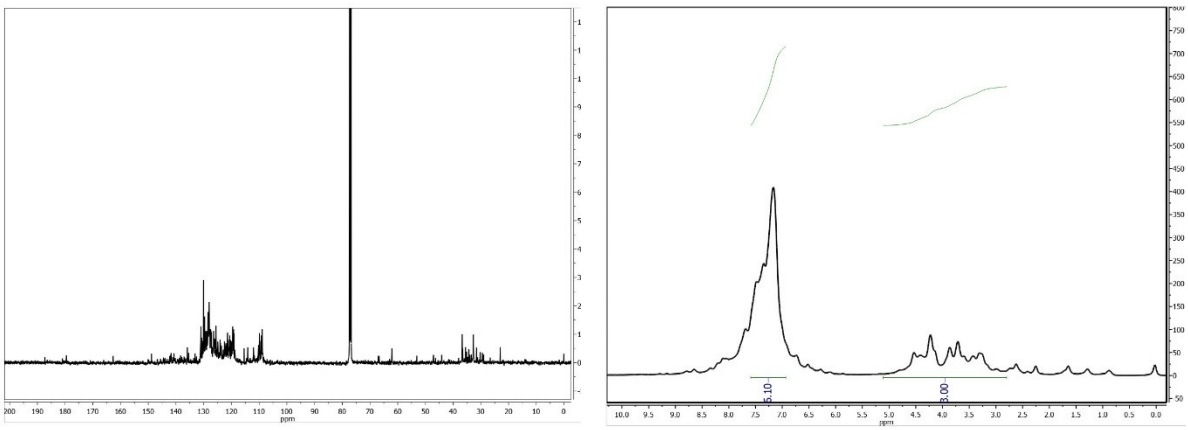

Figure 4. (a) ^{1}H NMR and (b) ^{13}C NMR spectra of PMPy.

Figure 5 shows the IR spectra of NMPy and PMPy. Similar to NMR spectra, clear broadening in the aliphatic and aromatic C-H stretching peaks points out successful polymerization. Minor changes in the fingerprint region might be due to the presence of high conjugation and dopant ions.

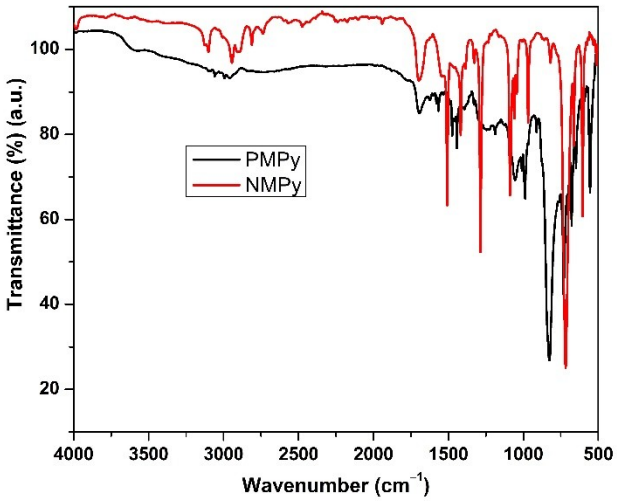

Figure 5. IR spectra of (red)NMPy and (black)PMPy.

In view of the previous laser-flash photolysis results obtained (38), the photopolymerization of NMPy should initiate by the formation of NMPy radical cation through photoinduced electron transfer (PET) within the excited complex (exciplex) formed between DPI and NMPy by irradiation. This is followed by the formation of dimer by coupling of two NMPy radical cations releasing HPF_6 acid. Since the oxidation of dimer is easier than the oxidation of monomer the photopolymerization proceeds through successive PET, coupling and acid release yielding PMPy doped with PF_6^- ion in a step-growth manner (Scheme 1).

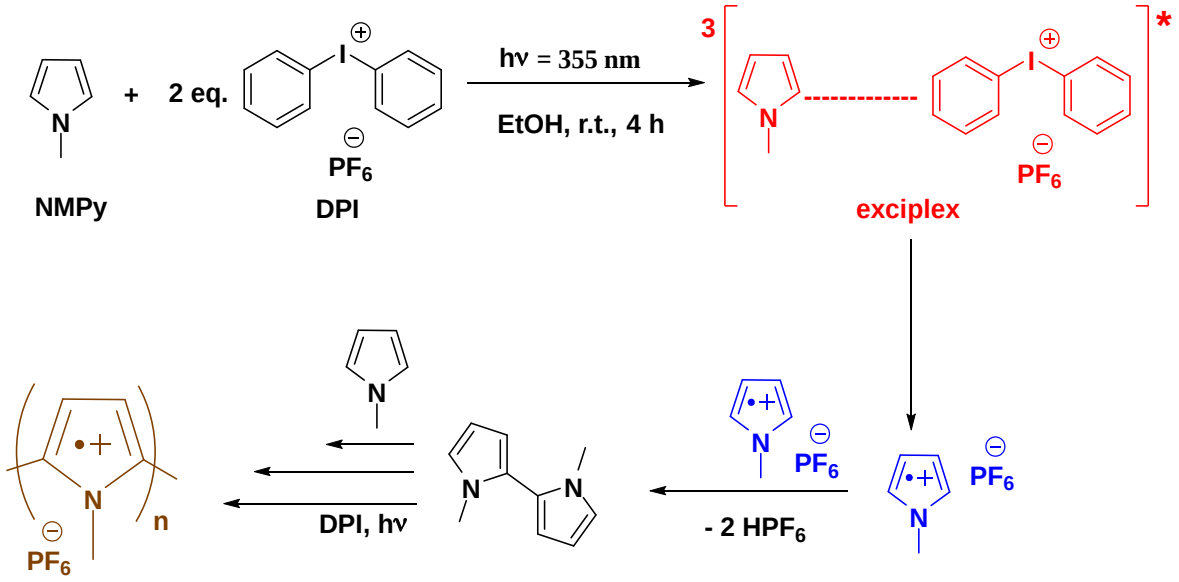

Scheme 1. Plaused mechanism for the photoinduced step-growth polymerization NMPy.

DSC thermogram of PMPy, similar to the literature results, shows no endotherms but two exotherms around 170 °C and 325 °C indicating recrystallization and degradation of the polymer, respectively. (Figure 6a). Thermal stability of the PMPy was also probed using TGA (Figure 6b). PMPy was stable (first 5% loss by weight) until 175 °C where after a sudden loss of weight occurred due to the removal of dopant ions and the gradual

degradation of polymeric chains, as previously observed in another photochemically polymerized *N*-methylpyrrole and *N*-methylindole using phenacyl bromide (38). The attribution of the first weight loss to the removal of dopant ions is due to the fact that the TGA thermogram of dedoped state of similar conjugated polymers (dedoped PEDOT) were previously shown to be thermally stable until the degradation point (39). When DSC and TGA results of PMPy are compared, it is possible to conclude that the two exothermic peaks in the DSC thermogram correspond to two major weight loss temperatures in TGA thermogram of PMPy.

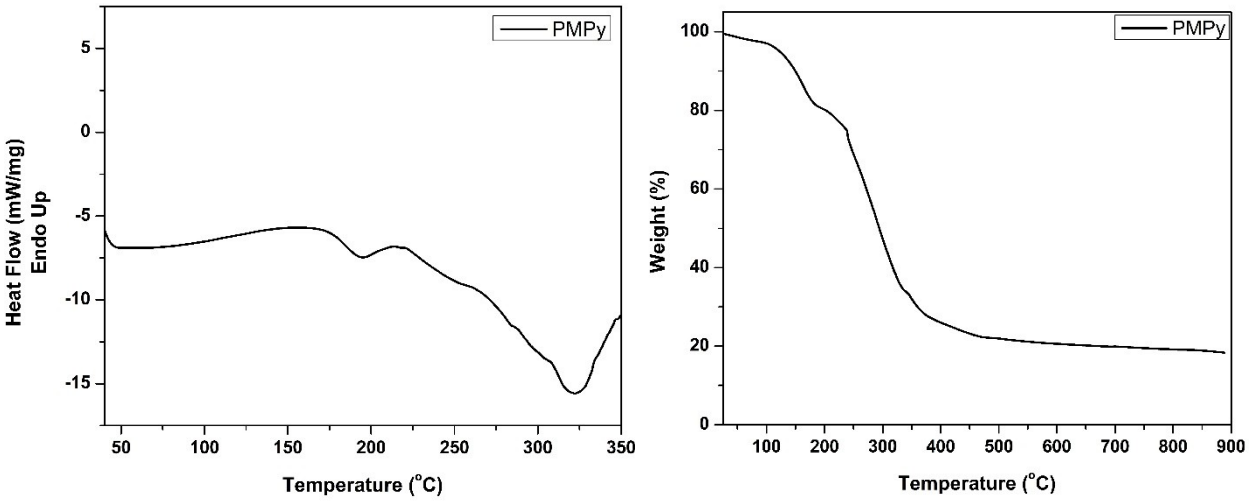

Figure 6. (a) DSC thermogram and (b) TGA thermogram of PMPy.

PXRD diffractogram of PMPy exhibited a totally amorphous nature and was in good agreement with the GPC traces indicating high molecular weight species (Figure 7). The peak around 2θ = 24° corresponds to - stacking between the pyrrole units of PMPy (40). The HOMO and LUMO level of the PMPy was calculated through its electrochemical data of three cycles obtained using cyclic voltammetry (CV) in acetonitrile solution (Figure 8) (HOMO = 1.00 eV (onset) and LUMO = -0.39 eV (onset)). Calculated electronic band gap of 1.39 eV is close to the previously obtained PMPy (1.45 eV) by photopolymerization method (38).

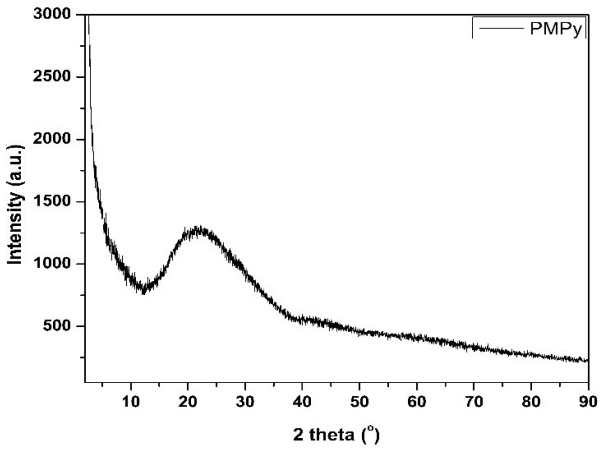

Figure 7. Powder X-Ray diffractogram of PMPy.

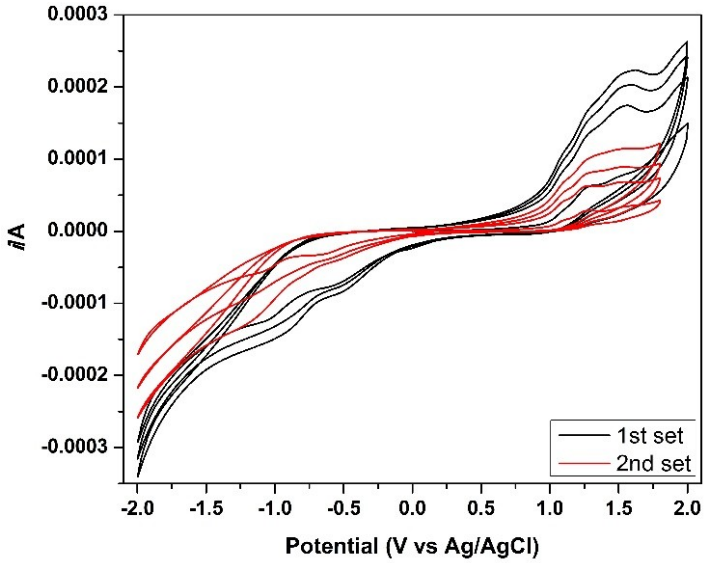

Figure 8. Cyclic voltammogram of PMPy.

4. CONCLUSION

In summary, high molecular weight poly (*N*-methylpyrrole) (PMPy) was photochemically obtained using DPI as one-component photoinitiator under green conditions. According to the previous experimental results obtained through the detection of acid and laser-flash photolysis, the photopolymerization should initiate by the oxidation of the monomer by DPI within the exciplex and should proceed with the coupling of two monomers forming dimer by releasing two protonic species. Propagation of the dimers and oligomers should go on in a step-growth manner finally terminated by hydrogen abstraction possibly from the solvent (EtOH). The method developed has many advantages over the conventional methods ((electro)chemical oxidation) such as the use of ambient conditions, green solvent, straightforward reaction procedure and short reaction time. Considering the strong electron acceptor feature of DPI, this work can be extended for the photopolymerization of other electron donor monomers.

5. CONFLICT OF INTEREST

The author declares no conflict of interest.

6. FUNDING

This work was supported by Istanbul Technical University Scientific Research Projects Coordination Unit.

7. ACKNOWLEDGEMENTS

The author thanks Prof. Yusuf Yagci for his supervision. This paper is dedicated to the memory of Prof. Yusuf Yagci.

8. REFERENCES

1. K N, Rout CS. Conducting polymers: a comprehensive review on recent advances in synthesis, properties and applications. RSC Advances. 2021;11(10):5659-97. <URL>

2. Nezakati T, Seifalian A, Tan A, Seifalian AM. Conductive Polymers: Opportunities and Challenges in Biomedical Applications. Chemical Reviews. 2018;118(14):6766-843. <URL>

3. Prunet G, Pawula F, Fleury G, Cloutet E, Robinson AJ, Hadziioannou G, et al. A review on conductive polymers and their hybrids for flexible and wearable thermoelectric applications. Materials Today Physics. 2021;18:100402. <URL>

4. R. Murad A, Iraqi A, Aziz SB, N. Abdullah S, Brza MA. Conducting Polymers for Optoelectronic Devices and Organic Solar Cells: A Review. Polymers. 2020;12(11):2627. <URL>

5. Heck J, Goding J, Portillo Lara R, Green R. The influence of physicochemical properties on the processibility of conducting polymers: A bioelectronics perspective. Acta Biomaterialia. 2022;139:259-79. <URL>

6. Wu X, Fu W, Chen H. Conductive Polymers for Flexible and Stretchable Organic Optoelectronic Applications. ACS Applied Polymer Materials. 2022;4(7):4609-23. <URL>

7. Aradilla D, Estrany F, Casellas F, Iribarren JI, Alemán C. All-polythiophene rechargeable batteries. Organic Electronics. 2014;15(1):40-6. <URL>

8. Yuan X, Zhao Y, Xie D, Pan L, Liu X, Duan C, et al. Polythiophenes for organic solar cells with efficiency surpassing 17%. Joule. 2022;6(3):647-61. <URL>

9. Langer JJ, Ratajczak K, Frąckowiak E, Golczak S. Water-Induced Tuning of the Emission of Polyaniline LEDs within the NIR to Vis Range. ACS Omega. 2021;6(50):34650-60. <URL>

10. Huang Y, Li H, Wang Z, Zhu M, Pei Z, Xue Q, et al. Nanostructured Polypyrrole as a flexible electrode material of supercapacitor. Nano Energy. 2016;22:422-38. <URL>

11. Sengodu P. 12 - Conjugated polymers-based biosensors. In: Kumar V, Sharma K, Sehgal R, Kalia S, editors. Conjugated Polymers for Next-Generation Applications. 1: Woodhead Publishing; 2022. p. 401-46. <URL>

12. Thadathil A, Pradeep H, Joshy D, Ismail YA, Periyat P. Polyindole and polypyrrole as a sustainable platform for environmental remediation and sensor applications. Materials Advances. 2022;3(7):2990-3022. <URL>

13. Pang AL, Arsad A, Ahmadipour M. Synthesis and factor affecting on the conductivity of polypyrrole: a short review. Polymers for Advanced Technologies. 2021;32(4):1428-54. <URL>

14. Tüken T, Tansuğ G, Yazıcı B, Erbil M. Poly(N-methyl pyrrole) and its copolymer with pyrrole for mild steel protection. Surface and Coatings Technology. 2007;202(1):146-54. <URL>

15. Elibal F, Gumustekin S, Ozkazanc H, Ozkazanc E. Poly(N-methylpyrrole) with high antibacterial activity synthesized via interfacial polymerization method. Journal of Molecular Structure. 2021;1242:130712. <URL>

16. Su W, Iroh JO. Electrodeposition mechanism, adhesion and corrosion performance of polypyrrole and poly(N-methylpyrrole) coatings on steel substrates. Synthetic Metals. 2000;114(3):225-34. <URL>

17. Branzoi F, Mihai MA, Petrescu S. Corrosion Protection Efficacy of the Electrodeposit of Poly (N-Methyl Pyrrole-Tween20/3-Methylthiophene) Coatings on Carbon Steel in Acid Medium. Coatings. 2022;12(8):1062. <URL>

18. Duran B, Bereket G. Cyclic Voltammetric Synthesis of Poly(N-methyl pyrrole) on Copper and Effects of Polymerization Parameters on Corrosion Performance. Industrial & Engineering Chemistry Research. 2012;51(14):5246-55.<URL>

19. Ahmad S. Electropolymerization of poly(methyl pyrrole)/carbon nanotubes composites derived from ionic liquid. Polymer Engineering & Science. 2009;49(5):916-21.<URL>

20. Huddleston JG, Visser AE, Reichert WM, Willauer HD, Broker GA, Rogers RD. Characterization and comparison of hydrophilic and hydrophobic room temperature ionic liquids incorporating the imidazolium cation. Green Chemistry. 2001;3(4):156-64. <URL>

21. Ustamehmetoğlu B, Kelleboz E. Oxidative Copolymerization of Pyrrole and N-Methyl Pyrrole. International Journal of Polymer Analysis and Characterization - Int J Polym Anal Charact. 2003;8:255-68. <URL>

22. Dubitsky YA, Zhubanov BA, Maresch GG. Synthesis of polypyrroles in the presence of ferric tetrafluoroborate. Synthetic Metals. 1991;41(1):373-6. <URL>

23. González-Tejera MJ, Martín G. Electrogeneration of Poly-N-Methylpyrrole Tosylate Doped Films. Electrochemical and Morphological Study. Portugaliae Electrochimica Acta. 2007;25:349-61. <URL>

24. Genies EM, Syed AA. Polypyrrole and poly N-methylpyrrole — An electrochemical study in an aqueous medium. Synthetic Metals. 1984;10(1):21-30. <URL>

25. Mahmoudian MR, Basirun WJ, Alias Y. Synthesis and characterization of poly(N-methylpyrrole)/TiO2 composites on steel. Applied Surface Science. 2011;257(8):3702-8. <URL>

26. Kaya K, Yagci Y. Contemporary Approaches for Conventional and Light-Mediated Synthesis of Conjugated Heteroaromatic Polymers. Macromolecular Chemistry and Physics. 2021;222(24):2100334. <URL>

27. Bagheri A, Jin J. Photopolymerization in 3D Printing. ACS Applied Polymer Materials. 2019;1(4):593-611. <URL>

28. Zou D, Nunes SP, Vankelecom IFJ, Figoli A, Lee YM. Recent advances in polymer membranes employing non-toxic solvents and materials. Green Chemistry. 2021;23(24):9815-43. <URL>

29. Somers P, Liang Z, Johnson JE, Boudouris BW, Pan L, Xu X. Rapid, continuous projection multi-photon 3D printing enabled by spatiotemporal focusing of femtosecond pulses. Light: Science & Applications. 2021;10(1):199. <URL>

30. Malik MS, Schlögl S, Wolfahrt M, Sangermano M. Review on UV-Induced Cationic Frontal Polymerization of Epoxy Monomers. Polymers. 2020;12(9):2146. <URL>

31. Shirai M. Photoinitiated Polymerization. In: Kobayashi S, Müllen K, editors. Encyclopedia of Polymeric Nanomaterials. Berlin, Heidelberg: Springer Berlin Heidelberg; 2015. p. 1579-85. <URL>

32. Sari E, Yilmaz G, Koyuncu S, Yagci Y. Photoinduced Step-Growth Polymerization of N-Ethylcarbazole. Journal of the American Chemical Society. 2018;140(40):12728-31. <URL>

33. Kaya K, Koyuncu S, Yagci Y. Photoinduced synthesis of poly(N-ethylcarbazole) from phenacylium salt without conventional catalyst and/or monomer. Chemical Communications. 2019;55(77):11531-4. <URL>

34. Yagci Y, Jockusch S, Turro NJ. Mechanism of Photoinduced Step Polymerization of Thiophene by Onium Salts: Reactions of Phenyliodinium and Diphenylsulfinium Radical Cations with Thiophene. Macromolecules. 2007;40(13):4481-5. <URL>

35. Celiker T, İsci R, Kaya K, Ozturk T, Yagci Y. Photoinduced step-growth polymerization of thieno[3,4-b] thiophene derivatives. The substitution effect on the reactivity and electrochemical properties. Journal of Polymer Science. 2020;58(17):2327-34. <URL>

36. Hebert DD, Naley MA, Cunningham CC, Sharp DJ, Murphy EE, Stanton V, et al. Enabling Conducting Polymer Applications: Methods for Achieving High Molecular Weight in Chemical Oxidative Polymerization in Alkyl- and Ether-Substituted Thiophenes. Materials (Basel). 2021;14(20):6146. <URL>

37. Abel SB, Frontera E, Acevedo D, Barbero CA. Functionalization of Conductive Polymers through Covalent Postmodification. Polymers. 2022;15(1):205. <URL>

38. Kocaarslan A, Kaya K, Jockusch S, Yagci Y. Phenacyl Bromide as a Single-Component Photoinitiator: Photoinduced Step-Growth Polymerization of N-Methylpyrrole and N-Methylindole. Angewandte Chemie International Edition. 2022;61(36):e202208845. <URL>

39. Kaya K. A green and fast method for PEDOT: Photoinduced step-growth polymerization of EDOT. Reactive and Functional Polymers. 2023;182:105464. <URL>

40. Celiker T, Kaya K, Koyuncu S, Yagci Y. Polypyrenes by Photoinduced Step-Growth Polymerization. Macromolecules. 2020;53(14):5787-94. <URL>